

# Glass-Encapsulated Light Harvesters: More Efficient Dye-Sensitized Solar Cells by Deposition of Self-Aligned, Conformal, and Self-Limited Silica Layers

Ho-Jin Son,<sup>†,||</sup> Xinwei Wang,<sup>‡,||</sup> Chaiya Prasittichai,<sup>†</sup> Nak Cheon Jeong,<sup>†</sup> Titta Aaltonen,<sup>‡,†</sup> Roy G. Gordon,<sup>\*,‡</sup> and Joseph T. Hupp<sup>\*,†,§</sup>

<sup>†</sup>Department of Chemistry and Argonne-Northwestern Solar Energy Research (ANSER) Center, Northwestern University, Evanston, Illinois 60208, United States

<sup>‡</sup>Department of Chemistry and Chemical Biology, Harvard University, Cambridge, Massachusetts 02138, United States

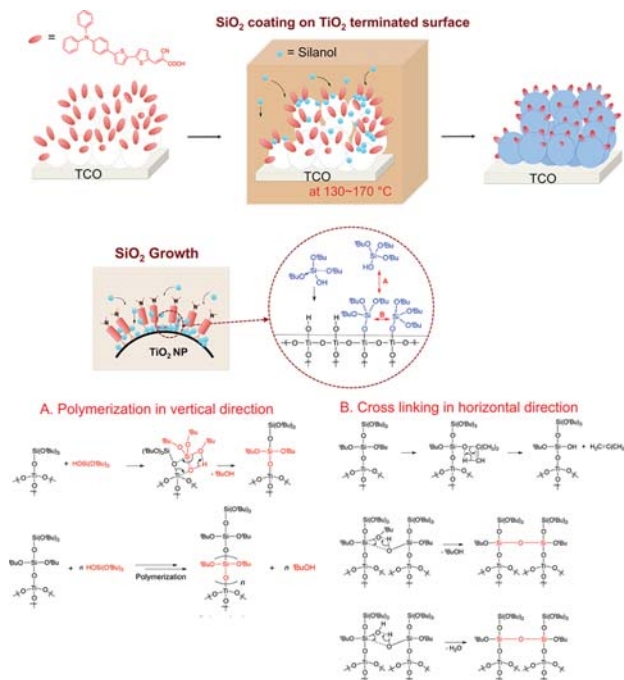
<sup>§</sup>Argonne National Laboratory, Argonne, Illinois 60439, United States

**S** Supporting Information

**ABSTRACT:** A major loss mechanism in dye-sensitized solar cells (DSCs) is recombination at the TiO<sub>2</sub>/electrolyte interface. Here we report a method to reduce greatly this loss mechanism. We deposit insulating and transparent silica (SiO<sub>2</sub>) onto the open areas of a nanoparticulate TiO<sub>2</sub> surface while avoiding any deposition of SiO<sub>2</sub> over or under the organic dye molecules. The SiO<sub>2</sub> coating covers the highly convoluted surface of the TiO<sub>2</sub> conformally and with a uniform thickness throughout the thousands of layers of nanoparticles. DSCs incorporating these selective and self-aligned SiO<sub>2</sub> layers achieved a 36% increase in relative efficiency versus control uncoated cells.

Dye-sensitized solar cells (DSCs) have great potential to compete with conventional p–n junction solar cells due to their relatively low cost.<sup>1</sup> However, their efficiency is limited by the ease with which electrons collected by the nanoparticle (NP) framework can recombine with ions in solution. Therefore, the photovoltaic efficiency of DSCs can be increased by retarding electron recombination at the photoelectrode interfaces. The surfaces of the TiO<sub>2</sub> NPs are not fully covered by the dye molecules, as shown schematically in Scheme 1. Thus, an electrical short by direct contact between electrolyte and the areas of TiO<sub>2</sub> not covered by dye provides an important loss pathway by which electrons recombine with the electrolyte. This recombination rate could be reduced or eliminated by selectively coating an insulating and transparent layer on these open areas of TiO<sub>2</sub>. In an effort to minimize such losses, many groups have proposed device architectures that include the coating of inorganic barrier layers,<sup>2</sup> the use of long aliphatic chain on organic framework,<sup>3</sup> saccharides,<sup>4</sup> the introduction of co-adsorbents,<sup>5</sup> encapsulation by cyclodextrins,<sup>6</sup> and post-surface passivation by polymerization.<sup>7</sup> Recently, high band gap metal oxide layers prepared via atomic layer deposition (ALD) have received much attention as efficient interface engineering tools owing to their capability of infiltrating porous structures, thereby ensuring good coverage of the surface of the nanoporous electrode,<sup>8</sup> fine control of thickness,<sup>9</sup> and low-temperature processing.<sup>10</sup> However,

**Scheme 1.** Post-dye SiO<sub>2</sub> Deposition Process and Plausible Reaction Mechanism on Dye-Coated TiO<sub>2</sub> Nanoparticles



applying ALD layers prior to dye adsorption on TiO<sub>2</sub> or related oxides significantly reduces the electron-transfer rate from the dye through the metal oxide overlayers by creating a tunneling barrier.<sup>11</sup> Therefore, a new methodology is needed that does not interfere with electron transfer to or from the dye molecules.

We discovered a method to deposit selectively an insulating and transparent layer of silica (SiO<sub>2</sub>) only on the open areas of TiO<sub>2</sub> surface, but not on the adsorbed dye molecules or between the dye surface-linker and the electrode. Our approach exploits deposition of SiO<sub>2</sub> from a precursor that is catalytically

**Received:** January 2, 2012

**Published:** June 1, 2012

decomposed by the surface of TiO<sub>2</sub>. Areas of TiO<sub>2</sub> covered by adsorbed dye do not catalyze the deposition of SiO<sub>2</sub>. Thus the gaps between dye molecules are selectively covered by SiO<sub>2</sub>. This SiO<sub>2</sub> retards the interfacial charge recombination dynamics without hindering electron injection from the dye into the TiO<sub>2</sub> or from the solution into the dye. When this SiO<sub>2</sub> treatment was applied to a DSC just after coating the TiO<sub>2</sub> with an organic dye (**OrgD**, Scheme 1), enhanced performance was obtained, with a higher power conversion efficiency and longer electron lifetime. Another important feature of the SiO<sub>2</sub> deposition process is that its thickness is self-limiting, so the same thickness is applied to all levels in the porous multilayer structure of the photoelectrode. In this study, we investigated the conditions needed to make SiO<sub>2</sub> deposit selectively on TiO<sub>2</sub> between dyes.

We found that SiO<sub>2</sub> less than 1 nm thick functions as a barrier to charge recombination and thereby improves the performance of these photovoltaic devices. The SiO<sub>2</sub> coating chemistry is related to a process for rapid ALD using alternating exposure of surfaces to vapors of trimethylaluminum (TMA) as a catalyst and tris(*tert*-butoxy)silanol (TBOS) as the SiO<sub>2</sub> precursor.<sup>12</sup> In this reaction, aluminum placed on the surface by the TMA plays a crucial role as a Lewis-acidic catalyst for deposition of SiO<sub>2</sub> layers up to 15 nm thick on top of the alumina.<sup>13</sup> There have been reports that hafnium and zirconium can also catalyze the growth of SiO<sub>2</sub>.<sup>14–16</sup> This work suggested to us that titanium might also catalyze the growth of SiO<sub>2</sub>. Indeed, we have found that anatase titanium dioxide does, in fact, catalyze growth of SiO<sub>2</sub> on its surface.

The SiO<sub>2</sub> coating process was performed in a home-built hot-wall tubular reactor (Scheme 1). TBOS was used as the precursor for both the silicon and the oxygen. The thickness of SiO<sub>2</sub> deposited on planar witness samples of TiO<sub>2</sub> is plotted as a function of substrate temperature in Figure 1. The reaction

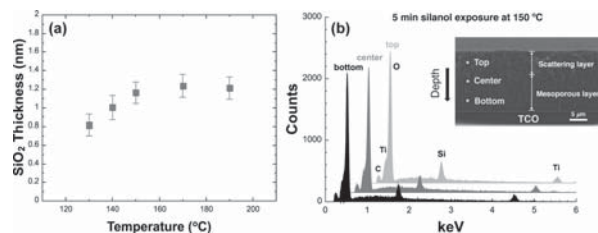


**Figure 1.** (a) RBS data for the thickness of the SiO<sub>2</sub> layer as a function of deposition temperature. (b) EDS data showing that the SiO<sub>2</sub> is deposited uniformly throughout the porous, nanoparticulate TiO<sub>2</sub> electrode.

temperature was varied from 130 to 190 °C, since no SiO<sub>2</sub> film was deposited below 130 °C. The amount of SiO<sub>2</sub> deposited was measured by the Rutherford backscattering spectroscopy (RBS) technique. The thickness of the SiO<sub>2</sub> film was found to increase with temperature from 0.8 nm to about 1.2 nm. These thicknesses represent the self-limited values obtained after initial dosing of about 1 Torr of silanol vapor, which was then allowed to react for 5 min. Other experiments showed that almost all of this deposition occurs within the first 10 s. Energy-dispersive X-ray spectroscopic (EDS) analyses (Figure 1) showed that the SiO<sub>2</sub> is evenly distributed throughout the thousands of TiO<sub>2</sub> NP layers constituting the photoanode. The coverage and thickness of the SiO<sub>2</sub> layer on the TiO<sub>2</sub> NPs were further examined with HRTEM (see Figure 2), which also

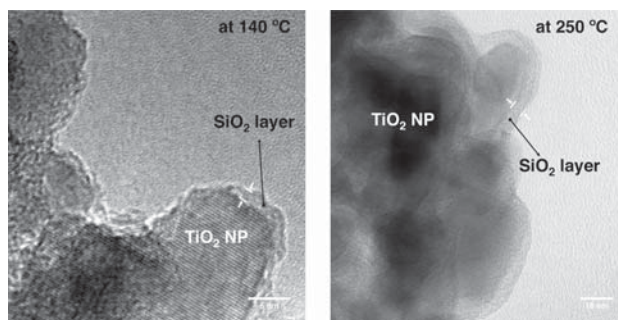


**Figure 2.** TEM images of TiO<sub>2</sub> NPs coated with SiO<sub>2</sub> at substrate temperatures of 140 and 250 °C.

shows a uniform and conformal SiO<sub>2</sub> layer. The thickness of the SiO<sub>2</sub> layer was ~1 and ~3 nm at 140 and 250 °C, respectively, showing the temperature dependence of the thickness, consistent with thicknesses determined by RBS.

Although it is not ideal to compare the thickness of SiO<sub>2</sub> on the dye-loaded TiO<sub>2</sub> surface with that on a flat surface, it should be noted that the real thickness of SiO<sub>2</sub> deposited is similar to the vertical dimension of dye molecules as evidenced by the stable oxidation of dyes within TiO<sub>2</sub>/SiO<sub>2</sub> films (Figure S1) and the corresponding *I*–*V* performance studied below (see Table 1). (Thicker layers might shut-off dye electrochemistry.)

**Table 1. Photovoltaic Performance of DSCs**

sample	$J_{sc}$ [mA/cm <sup>2</sup> ]	$V_{oc}$ [V]	ff	$\eta$ [%]
OrgD	9.95	0.62	0.71	4.36
OrgD/(SiO <sub>2</sub> ) <sub>130</sub>	11.03	0.66	0.69	5.02
OrgD/(SiO <sub>2</sub> ) <sub>140</sub>	12.63	0.69	0.68	5.94
OrgD/(SiO <sub>2</sub> ) <sub>150</sub>	12.17	0.68	0.69	5.70
OrgD/(SiO <sub>2</sub> ) <sub>170</sub>	12.07	0.67	0.65	5.29
N719	13.58	0.77	0.71	7.39

In UV/vis spectra of TiO<sub>2</sub>/OrgD/SiO<sub>2</sub> films, no significant decrease in absorbance is observed after SiO<sub>2</sub> deposition, indicating the sensitizing dye molecules are not affected by the SiO<sub>2</sub> precursor or the thermal stress during SiO<sub>2</sub> deposition (Figures S2 and S3). Given the fact that the sensitized dye molecules are partly surrounded by the SiO<sub>2</sub> layer, resulting in a change of the external dielectric field, the unchanged  $\lambda_{max}$  in the films arises from the low dielectric constant of SiO<sub>2</sub> ( $\epsilon \approx 4$ ), which acts as a nonpolar medium.

Enshrouding dyes with a glass (SiO<sub>2</sub>) coating of precise and uniform thickness substantially improves the photovoltaic performance of the DSC devices. Figure 3 shows action spectra in the form of monochromatic incident photon-to-current conversion efficiencies (IPCEs) for DSCs based on **OrgD** (electrolyte: 0.6 M DMPImI, 0.05 M iodine, 0.1 M LiI, and 0.5 M *tert*-butylpyridine in acetonitrile). The post-dye-treated **OrgD**/(SiO<sub>2</sub>)<sub>*x*</sub> (*x* = SiO<sub>2</sub> deposition temperature ranging from 130 to 170 °C) cells clearly exhibited an increased response over the entire spectral region, but especially the red region, relative to the nontreated **OrgD** cell. The IPCE of **OrgD**/(SiO<sub>2</sub>)<sub>130–170</sub> showed plateaus of over 75% from 400 to 590 nm. Significantly higher responses were observed over the wavelength range of 500–700 nm for **OrgD**/(SiO<sub>2</sub>)<sub>130–170</sub> cells compared to **OrgD** cell. The broadened IPCEs of these coated cells suggest superior electron collection capability (greater collection length) versus untreated cells. If we examine IPCE as

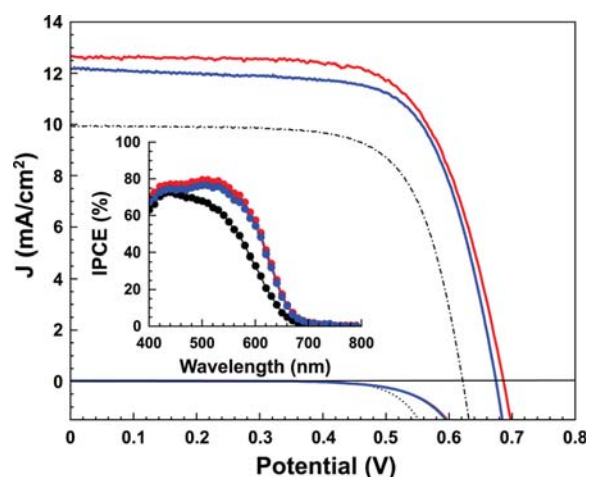


**Figure 3.**  $J$ - $V$  curves, dark currents, and IPCE plots (inset) of **OrgD** (black dashed line), **OrgD**/(SiO<sub>2</sub>)<sub>140</sub> (red line), and **OrgD**/(SiO<sub>2</sub>)<sub>150</sub> (blue line).

a function of light harvesting efficiency over the wavelength (Figure S4), the results suggest that the coated films have much longer *effective* light infiltration compared to uncoated ones (“effective” means ability to inject electrons that are subsequently collected as a photocurrent rather than lost to interception by I<sub>3</sub><sup>−</sup> or recombination with oxidized dye). An additional minor contributor to the IPCE broadening could be a red shift in dye absorption following encapsulation. Extinction measurements suggest that, depending on the wavelength, the shift could be as large as 15 nm. The measurements were complicated, however, by baseline shifts presumably due to light scattering.

The photovoltaic performances of the **OrgD** sensitized cells are listed in Table 1.<sup>17</sup> The optimal condition for the SiO<sub>2</sub> barrier was that produced at 140 °C (~1.0 nm by RBS), which resulted in 36% increase in efficiency ( $\eta$ ) compared to the reference cell, with the highest  $\eta$  achieved being 5.94%; both the open-circuit photovoltage ( $V_{oc}$ ) value of 0.69 V and the short-circuit photocurrent ( $J_{sc}$ ) value of 12.63 mA/cm<sup>2</sup> are larger than for the uncoated control.<sup>18</sup> This value agrees well with that obtained by integrating solar-spectrum-weighted IPCE. Under the same conditions, the **OrgD** cell gave  $J_{sc}$  = 9.95 mA/cm<sup>2</sup>,  $V_{oc}$  = 0.62 V, and fill-factor ( $ff$ ) = 0.71, which correspond to  $\eta$  = 4.36%. When the deposition temperature was increased to 150 °C, the resulting device showed slightly poorer characteristics than the **OrgD**/(SiO<sub>2</sub>)<sub>140</sub> cell. Of particular importance is the 60–70 mV increase in the  $V_{oc}$  value of the **OrgD**/(SiO<sub>2</sub>)<sub>130–170</sub> cell relative to the **OrgD** cell. This result implies that the SiO<sub>2</sub> surrounding the dye results in retardation of interfacial charge recombination losses in the device, as confirmed by the dark current data (Figure 3). Charge lifetimes ( $\tau_e$ ) determined from  $V_{oc}$  decay measurements are shown in Figure 4a. The  $\tau_e$  values are successively shifted to larger values with increase of reaction temperature from 130 to 170 °C, demonstrating that the electron-recombination process was effectively retarded by the SiO<sub>2</sub> deposition. Specifically, the increase of  $\tau_e$  by the post-dye SiO<sub>2</sub> layer is saturated with the amount produced at 140 °C, showing that as little as 1.0 nm of SiO<sub>2</sub> (about 4 monolayers) is sufficient to insulate the TiO<sub>2</sub> surfaces very efficiently. These results are also in good agreement with the  $V_{oc}$  results shown in Table 1.

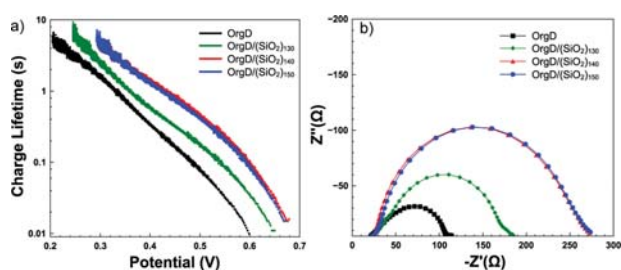


**Figure 4.** (a) Charge lifetimes from open-circuit photovoltage decays. (b) Dark electrochemical impedance spectra at 575 mV of **OrgD**, **OrgD**/(SiO<sub>2</sub>)<sub>130</sub>, **OrgD**/(SiO<sub>2</sub>)<sub>140</sub>, and **OrgD**/(SiO<sub>2</sub>)<sub>150</sub> cells.

Electrochemical impedance spectroscopy (EIS) was performed under dark conditions (Figure 4b) with the forward bias ranging from −0.5 to −0.7 V. The semicircular curve obtained in the intermediate-frequency regime shows the dark reaction impedance caused by electron transport from the TiO<sub>2</sub> conduction band to the I<sub>3</sub><sup>−</sup> ions in the electrolyte.<sup>19</sup> The radius of the intermediate frequency semicircle showed the increasing order of **OrgD** (72 Ω) < **OrgD**/(SiO<sub>2</sub>)<sub>130</sub> (133 Ω) < **OrgD**/(SiO<sub>2</sub>)<sub>140</sub> (239 Ω) ≤ **OrgD**/(SiO<sub>2</sub>)<sub>150</sub> (241 Ω), which is in agreement with the trends of the  $V_{oc}$  and  $\tau_e$  values. EIS also revealed that the effective length of **OrgD**/(SiO<sub>2</sub>)<sub>140</sub> is roughly 2.5 times greater than that of **OrgD**, confirming that SiO<sub>2</sub> inhibits the interception of injected electrons by the I<sub>3</sub><sup>−</sup> ions in the electrolyte (Figure 5).<sup>20</sup> Figure S5 shows that the untreated

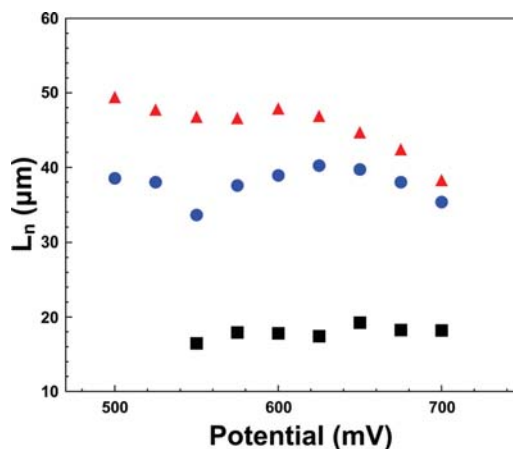


**Figure 5.** Effective electron diffusion lengths (from dark EIS) for the electrodes coated with **OrgD** (black squares), **OrgD**/(SiO<sub>2</sub>)<sub>140</sub> (red triangles), and **OrgD**/(SiO<sub>2</sub>)<sub>150</sub> (blue circles).

and treated cells have a similar capacitance, indicating that the band-edge of the nanoporous TiO<sub>2</sub> network is not affected by the SiO<sub>2</sub> deposition (Figure S5). We envision that this strategy could be even more useful for the bulky outer-sphere redox shuttles. Such studies are currently in progress and will be presented elsewhere.

In summary, we have demonstrated that self-aligned, conformal, and self-limiting deposition of SiO<sub>2</sub> on TiO<sub>2</sub> in DSCs is an effective tool for retarding charge recombination, leading to enhanced charge collection and substantially increased overall conversion efficiency. The SiO<sub>2</sub> layer forms only on the TiO<sub>2</sub> and does not cover the dye molecules. Moreover, this new architecture provides an insulating layer that retards interfacial charge recombination without reducing

electron transfer from the dye into the TiO<sub>2</sub> NPs or from the solution to the dye. Optimization of DSCs using this SiO<sub>2</sub> post-dye treatment as well as application to other, more strongly absorbing dyes is currently being investigated. We believe that the development of highly efficient DSC devices with excellent stabilities is possible through this interfacial engineering.

## ■ ASSOCIATED CONTENT

### ■ Supporting Information

Experimental conditions and results of cyclic voltammetry, UV/vis spectra,  $J$ - $V$  curves, chemical capacitance experiments, and TEM image. This material is available free of charge via the Internet at <http://pubs.acs.org>.

## ■ AUTHOR INFORMATION

### Corresponding Author

[gordon@chemistry.harvard.edu](mailto:gordon@chemistry.harvard.edu); [j-hupp@northwestern.edu](mailto:j-hupp@northwestern.edu)

### Present Address

<sup>+</sup>Centre for Materials Science and Nanotechnology, University of Oslo, Norway

### Author Contributions

<sup>||</sup>H.-J.S. and X.W. contributed equally.

### Notes

The authors declare no competing financial interest.

## ■ ACKNOWLEDGMENTS

Work in the R.G.G. group was performed in part at Harvard University's Center for Nanoscale Systems (CNS), a member of the National Nanotechnology Infrastructure Network (NNIN), which is supported by the National Science Foundation under NSF award no. ECS-0335765. Work at Northwestern University was supported as part of the ANSER Center, an Energy Frontier Research Center funded by the U.S. Department of Energy, Office of Science, Office of Basic Energy Sciences under Award No. DE-SC0001059. We also gratefully acknowledge the government of Thailand's Commission on Higher Education for providing partial graduate fellowship support for C.P. through its program on Strategic Fellowships for Frontier Research Networks, and the Yulchon Foundation in Korea for providing a research fellowship for partial support of H.-J.S. Finally, we thank a reviewer for insightful advice on validating  $\eta$  measurements.

## ■ REFERENCES

- (1) (a) O'Regan, B.; Grätzel, M. *Nature* **1991**, *353*, 737. (b) Grätzel, M. *Nature* **2001**, *414*, 338. (c) Wang, P.; Klein, C.; Humphry-Baker, R.; Zakeeruddin, S. M.; Grätzel, M. *J. Am. Chem. Soc.* **2005**, *127*, 808. (d) Robertson, N. *Angew. Chem., Int. Ed.* **2006**, *45*, 2338. (e) Ardo, S.; Meyer, G. J. *Chem. Soc. Rev.* **2009**, *38*, 115. (f) Hagfeldt, A.; Boschloo, G.; Sun, L.; Kloo, L.; Pettersson, H. *Chem. Rev.* **2010**, *110*, 6595.
- (2) (a) Palomares, E.; Clifford, J. N.; Haque, S. A.; Lutz, T.; Durrant, J. R. *J. Am. Chem. Soc.* **2003**, *125*, 475. (b) Clifford, J. N.; Yahioglu, G.; Milgrom, L. R.; Durrant, J. R. *Chem. Commun.* **2002**, 1260.
- (3) (a) Koumura, N.; Wang, Z.-S.; Mori, S.; Miyashita, M.; Suzuki, E.; Hara, K. *J. Am. Chem. Soc.* **2006**, *128*, 14256. (b) Choi, H.; Baik, C.; Kang, S. O.; Ko, J.; Kang, M.-S.; Nazeeruddin, M. K.; Grätzel, M. *Angew. Chem., Int. Ed.* **2008**, *47*, 327.
- (4) Handa, S.; Haque, S. A.; Durrant, J. R. *Adv. Funct. Mater.* **2007**, *17*, 2878.
- (5) (a) Kay, A.; Grätzel, M. *J. Phys. Chem. B* **1993**, *97*, 6272. (b) Schlichthörl, G.; Huang, S. Y.; Sprague, J.; Frank, A. J. *J. Phys. Chem. B* **1997**, *101*, 8141. (c) Wang, P.; Zakeeruddin, S. M.; Humphry-Baker, R.; Grätzel, M. *Chem. Mater.* **2004**, *16*, 2694.

(6) Choi, H.; Kang, S. O.; Ko, J.; Gao, G.; Kang, H. S.; Kang, M.-S.; Nazeeruddin, M. K.; Grätzel, M. *Angew. Chem., Int. Ed.* **2009**, *48*, 5938.

(7) (a) Feldt, S. M.; Cappel, U. B.; Johansson, E. M. J.; Boschloo, G.; Hagfeldt, A. *J. Phys. Chem. C* **2010**, *114*, 10551. (b) Park, S.-H.; Lim, J.; Song, I. Y.; Atmakuri, N.; Song, S.; Kwon, Y. S.; Choi, J. M.; Park, T. *Adv. Energy Mater.* **2012**, *2*, 219.

(8) (a) Scharrer, M.; Wu, X.; Yamilov, A.; Cao, H.; Chang, R. P. H. *Appl. Phys. Lett.* **2005**, *86*, 151113. (b) Law, M.; Greene, L. E.; Radenovic, A.; Kuykendall, T.; Liphardt, J.; Yang, P. *J. Phys. Chem. B* **2006**, *110*, 22652.

(9) (a) Ritala, M.; Leskelä, M. *Nanotechnology* **1999**, *10*, 19. (b) Niinistö, L.; Päiväsäari, J.; Niinistö, J.; Putkonen, M.; Nieminen, M. *Phys. Stat. Sol. (a)* **2004**, *201*, 1443.

(10) (a) Groner, M. D.; Fabreguette, F. H.; Elam, J. W.; George, S. M. *Chem. Mater.* **2004**, *16*, 639. (b) Hausmann, D. M.; Kim, E.; Becker, J.; Gordon, R. G. *Chem. Mater.* **2002**, *14*, 4350.

(11) (a) Hamann, T. W.; Farha, O. K.; Hupp, J. T. *J. Phys. Chem. C* **2008**, *112*, 19756. (b) Lin, C.; Tsai, F.-Y.; Lee, M.-H.; Lee, C.-H.; Tien, T.-C.; Wang, L.-P.; Tsai, S.-Y. *J. Mater. Chem.* **2009**, *19*, 2999. (c) Antila, L. J.; Heikkilä, M. J.; Aumanen, V.; Kemell, M.; Myllyperkiö, P.; Leskelä, M.; Korppi-Tommola, J. E. I. *J. Phys. Chem. Lett.* **2010**, *1*, 536. (d) Prasittichai, C.; Hupp, J. T. *J. Phys. Chem. Lett.* **2010**, *1*, 1611.

(12) Hausmann, D.; Becker, J.; Wang, S.; Gordon, R. G. *Science* **2002**, *298*, 402.

(13) Burton, B. B.; Boleslawski, M. P.; Desombre, A. T.; George, S. M. *Chem. Mater.* **2008**, *20*, 7031.

(14) (a) Gordon, R. G.; Becker, J.; Hausmann, D.; Suh, S. *Chem. Mater.* **2001**, *13*, 2463. (b) Zhong, L. J.; Daniel, W. L.; Zhang, Z. H.; Campbell, S. A.; Gladfelter, W. L. *Chem. Vap. Dep.* **2006**, *12*, 143.

(15) Zhong, L. J.; Zhang, Z. H.; Campbell, S. A.; Gladfelter, W. L. *J. Mater. Chem.* **2004**, *14*, 3203.

(16) He, W.; Solanki, R.; Conley, J. F.; Ono, Y. *J. Appl. Phys.* **2003**, *94*, 3657.

(17) During manuscript revision, a light-intensity-calibration error was discovered.  $J$ - $V$  measurements were found to have been made at 1.3 sun, rather than 1 sun (100 mW/cm<sup>2</sup>). (IPCE measurements were not affected by the error.) The photocurrent densities shown in Figure 3 and listed in Table 1 have been corrected downward by a factor of 1.3 to account for the error. It is conceivable that small errors in photovoltages remain. We have not attempted to correct for these.

(18) In contrast, the commonly utilized co-adsorbent, chenodeoxycholic acid (see ref S1 in SI), yielded no improvement in efficiency, indicating that here it is ineffective in preventing electrolyte interception of injected electrons.

(19) Wang, Q.; Moser, J.-E.; Grätzel, M. *J. Phys. Chem. B* **2005**, *109*, 14945.

(20) We have previously shown that polarizable organic dyes can form weak complexes with I<sub>3</sub><sup>-</sup>, thereby enhancing its local (i.e., interfacial) concentration: Splan, K. E.; Massari, A. M.; Hupp, J. T. *J. Phys. Chem. B* **2004**, *108*, 4111. See also: O'Regan, B. C.; et al. *J. Am. Chem. Soc.* **2008**, *130*, 2906. If complex formation is diminished or eliminated by dye encapsulation, this could be an additional means of inhibiting dark current.